Pergamon

Journal of Structural Geology, Vol. 16, No. 7, pp. 985 to 996, 1994

0191-8141/94 $07.00+0.00

Ductility of garnet as an indicator of extremely high temperature deformation

SHAOCHENG JI and JACQUES MARTIGNOLE*

Département de géologie, Université de Montréal, C.P. 6128, Succursale "A", Montréal, Québec, Canada H3C 3J7

(*Received* 18 *December* 1992; *accepted in revised form* 2 *September* 1993)

Abstract—Discoidal shaped garnets (Alm63 Prp33 Grs3 Sps1) occur in the foliation plane of lineated quartzo-feldspathic mylonites of the Morin shear zone located along the eastern boundary of the Morin anorthosite complex (Grenville Province, Quebec). The flattened shape of garnets records a component of coaxial strain ($X = Y \gg Z$), different from the dominant rotational shear strain ($X > Y > Z$) in this mylonite. TEM observations indicate dislocation slip and recovery to be the main mechanism for the deformation of garnet. Extrapolation of available experimentally-determined flow laws to natural strain-rates shows an inversion of flow strength between quartz ± feldspar and garnet: garnet, much stronger than quartz and feldspar at temperatures below 700°C, becomes weaker than quartz and feldspar above 900°C. The coaxial ductile strain recorded by the garnets could be produced by a local, uncharacterized deformation, under extremely high temperature conditions at the roof of the rising anorthositic diapir (~1155 Ma). Subsequent, lower temperature rotational deformation is related to strike-slip movement along the Morin shear zone (~1020 Ma).

INTRODUCTION

GARNET is a widespread metamorphic mineral in the middle and lower crust, and is likely to be one of the major mineral constituents in the subducting oceanic crust and in the transition zone of the mantle (Ringwood 1975, Anderson 1989). This mineral has received much attention for the following reasons: (i) garnet composition is a sensitive indicator of the metamorphic *P–T* path followed during mineral growth (e.g. Spear & Selverstone 1983); (ii) spiral-shaped inclusions in garnet porphyroblasts are indicators for rotational deformation (e.g. Spry 1983, Passchier *et al.* 1992) or for multiphase non-rotational deformations (Bell & Johnson 1989, Bell *et al.* 1992); and (iii) garnet as an isotopic chronometer can provide valuable information about rates of tectono-metamorphic processes (e.g. Christensen *et al.* 1989, Burton & O'Nions 1991). However, little is known about mechanical properties, especially about rheological behavior of garnet (Rabier *et al.* 1976, 1979, Garem *et al.* 1982, Smith 1982, Rabier & Garem 1984, Allen *et al.* 1987, Wang & Karato 1991, Wang *et al.* 1991, Liu *et al* 1992, Parthasarathy *et al.* 1992). So far as the authors are aware, there have been only three reports on the natural ductile deformation of garnet (Dalziel & Bailey 1968, Ross 1973, van Roermund 1989). In this paper, we give preliminary results of research on garnet ductility in granulite–amphibolite facies quartzo-feldspathic mylonites from the Morin anorthosite complex exposed in the Grenville Province, Quebec. The conditions for garnet deformation are discussed in the light of available data on the rheological properties of quartz, feldspar and garnet.

GEOLOGICAL SETTING

The Morin Anorthosite Massif is the core of a plutonic complex (Martignole & Schrijver 1970) emplaced around 1155 Ma (Doig 1991) in high-grade metamorphic rocks of the allochthonous monocyclic belt of the Grenville Province (Rivers *et al.* 1989). Along the least deformed margin of the anorthosite, the preservation of very high temperature minerals and assemblages like wollastonite–calcite in the marbles and corundum–quartz in aluminous quartzites attests for intense contact metamorphism. The eastern part of the massif along with its country rocks was mylonitized with W-dipping foliations and a sub-horizontal stretching lineation. This deformation was caused by dextral strike-slip ductile shear of the Morin shear zone (Fig. 1) which took place around 1020 Ma (Martignole & Friedman 1993). Rocks involved in this ductile shear zone are highly strained members of the anorthosite–norite suite, mylonitic charnockites or mylonitic metasediments including garnetiferous quartzo-feldspathic gneisses, metapelite and pyroxene amphibolite. Most of these rocks are characterized by a prominent mylonitic foliation usually dipping to the west but locally undulated in N–S trending open folds (Martignole & Schrijver 1970). Stretching lineations are defined by elongated pyroxene porphyroclasts in anorthositic rocks and by quartz and feldspar ribbons in quartzo-feldspathic rocks. When considered at the mesoscopic scale, a single deformation is visible in these highly strained rocks, namely the one related to N–S dextral shearing, with γ-values up to 10. The garnetiferous quartzo-feldspathic gneisses are characterized by interlayered compositional bands rich in, respectively,

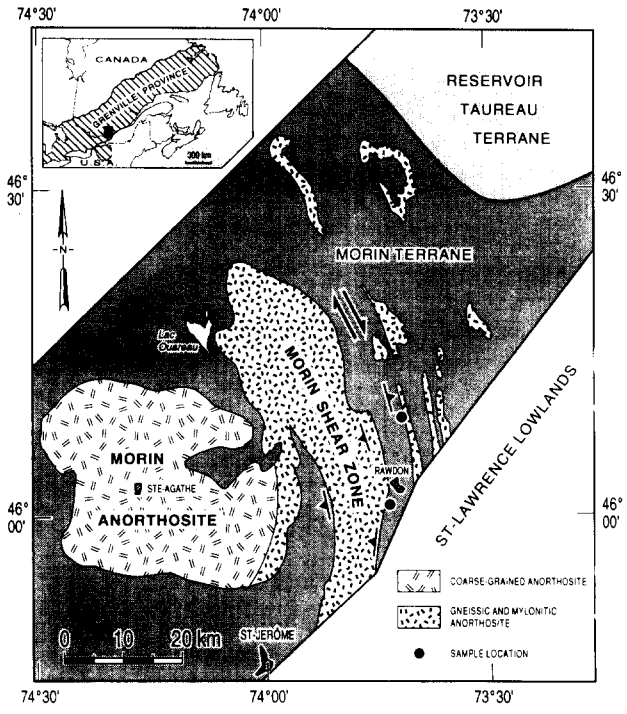

Fig. 1. Geological map of study area showing sample locaties.

quartz, feldspar + quartz, and locally pyroxene + garnet.

CHEMICAL COMPOSITION OF GARNET

A Camebax electron microprobe with an EDS system has been used for analyzing the chemical composition of garnets from the quartz-rich and feldspar-rich layers. The 129 analyses performed along four profiles in each grain show that oblate and equidimensional garnets have identical composition (Alm63 Prp33 Grs3 Sps1) and that there is no compositional variation from core to rim. The absence of compositional zoning in the garnets can be attributed to homogenization by effective diffusion at high temperature (Yardley 1977) and to the absence of exchange reactions between garnet and adjacent minerals during cooling. Since Fe–Mg minerals such as biotite are absent in the quartzo-feldspathic mylonite, retrograde compositional zoning could not develop and consequently garnet preserves its high temperature homogeneous composition.

MICROSTRUCTURES

Garnet

Garnet, which represents only 2–3 vol. % of the quartz-rich layers, is isolated in a ductilely deformed matrix of quartz (Figs. 2 and 3). In thin sections cut parallel to the lineation and perpendicular to the foliation (X–Z-section), garnet single crystals generally show a shape of elongate lenses with two smoothly curved boundaries subparallel to the foliation. Intersections of these two boundaries form two outward-pointing cusps extending into the foliation plane (Fig. 4). The aspect ratio of garnets in the X–Z section ranges from 1 to 9, with an average value of 3.1, the latter indicating an average strain of 50% if garnets are assumed to be equidimensional prior to deformation. Some garnet grains show a well developed pinch-and-swell structure (Fig. 4c). Measurements made on thin sections parallel to X–Z and X–Y planes show that the garnets are dimensionally flattened oblate spheroids with a Flinn coefficient (k) of 0.126 (Fig. 6a). Deflection of the foliation defined by feldspars and particularly quartz ribbons around garnets suggests that these garnets crystallized prior to the formation of the mylonitic foliation and lineation.

The garnets usually do not contain inclusions but where these occur, they are spherical quartz grains without optical evidence for intracrystalline strain such as undulatory extinction, lattice rotation and subgrain boundaries (Figs. 4a & e). The garnets in feldspar-rich layers are less flattened than those in the quartzite layers. There are two generations of tensile fractures in garnet single crystals. Both of them are planar cracks normal or subperpendicular to the lineation. Second generation fractures are ubiquitous in the sample and were formed during brittle deformation since they continuously cut both garnet and the quartz matrix (Fig. 4). The fractures of the first generation were developed during the stage when quartz was still deforming ductilely since they cut and pull-apart the outward-pointing cusps of garnet from the central main segment (Ji & Zhao 1993) (Figs. 2 and 4d–f). The gaps between garnet boudins and their pressure-shadow sites are filled with deformed quartz (Fig. 4d), feldspar (Fig. 4e) and magnetite. The first generation of tensile fractures is much less common than the second generation.

Unlike in feldspars and quartz, optical intracrystalline deformation features such as undulatory extinction, lattice bending and kink bending cannot be seen in isotropic garnet. Two techniques, transmission electron microscopy (TEM) and surface etching, were used in order to determine the possible mechanisms responsible for the observed ductile deformation of garnets. Dislocation structures in pyrope-rich garnets from peridotites were revealed by Carstens (1969, 1971) using the etching of thin polished slices in 20% hydrofluoric acid for 24 h at room temperature. However, our attempt to reveal dislocation channels in the almandine-rich garnet has so far failed. TEM observations were performed in a 200 kV accelerating voltage Jeol-Jem 2000 EX electron microscope at the Laboratoire de Métallurgie de l'Ecole Polytechnique, Université de Montréal. Single crystals of discoidal shaped garnet were selected from double-polished petrographic thin sections for thinning by ion bombardment using Ar^+ ions at 5 kV. TEM observations on deformed garnet grains show that the distribution of free dislocation densities is quite homogeneous. Both curved or straight dislocations are observed (Fig. 6). Measurements of representative

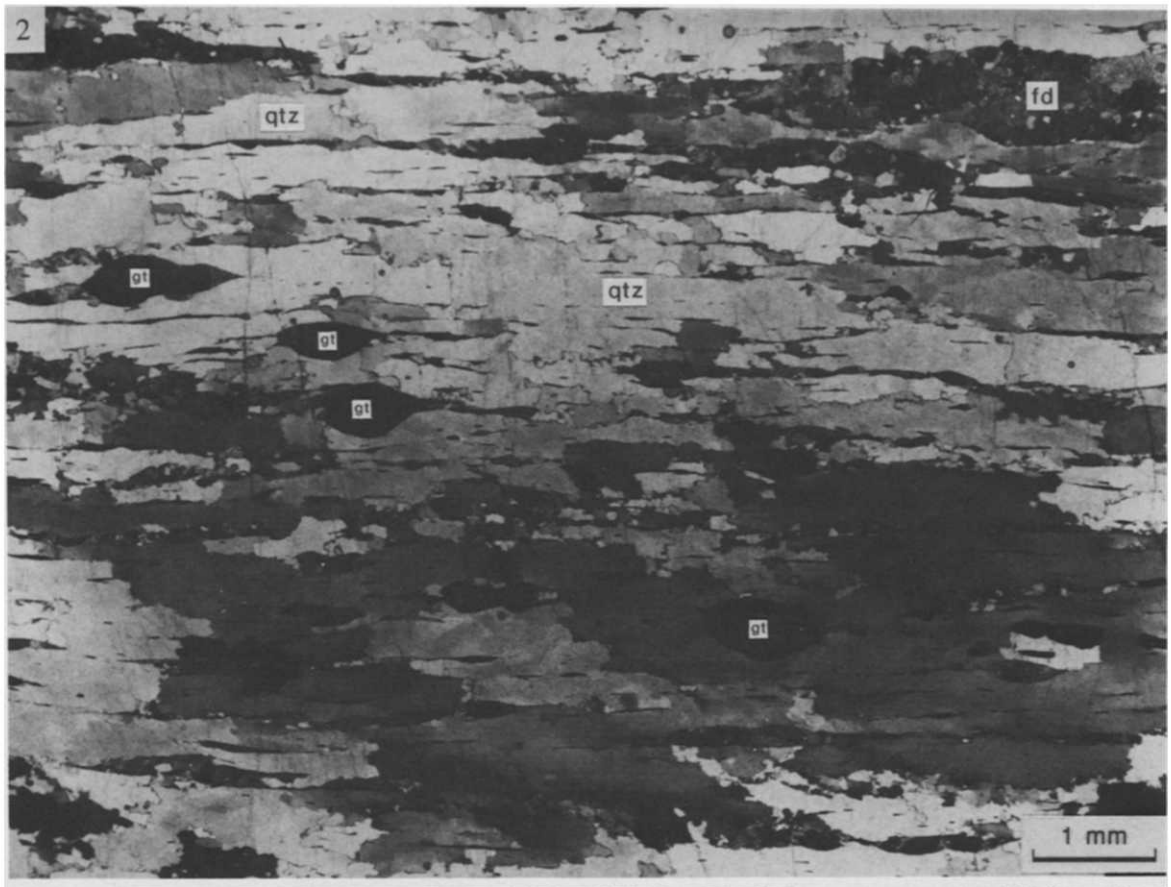

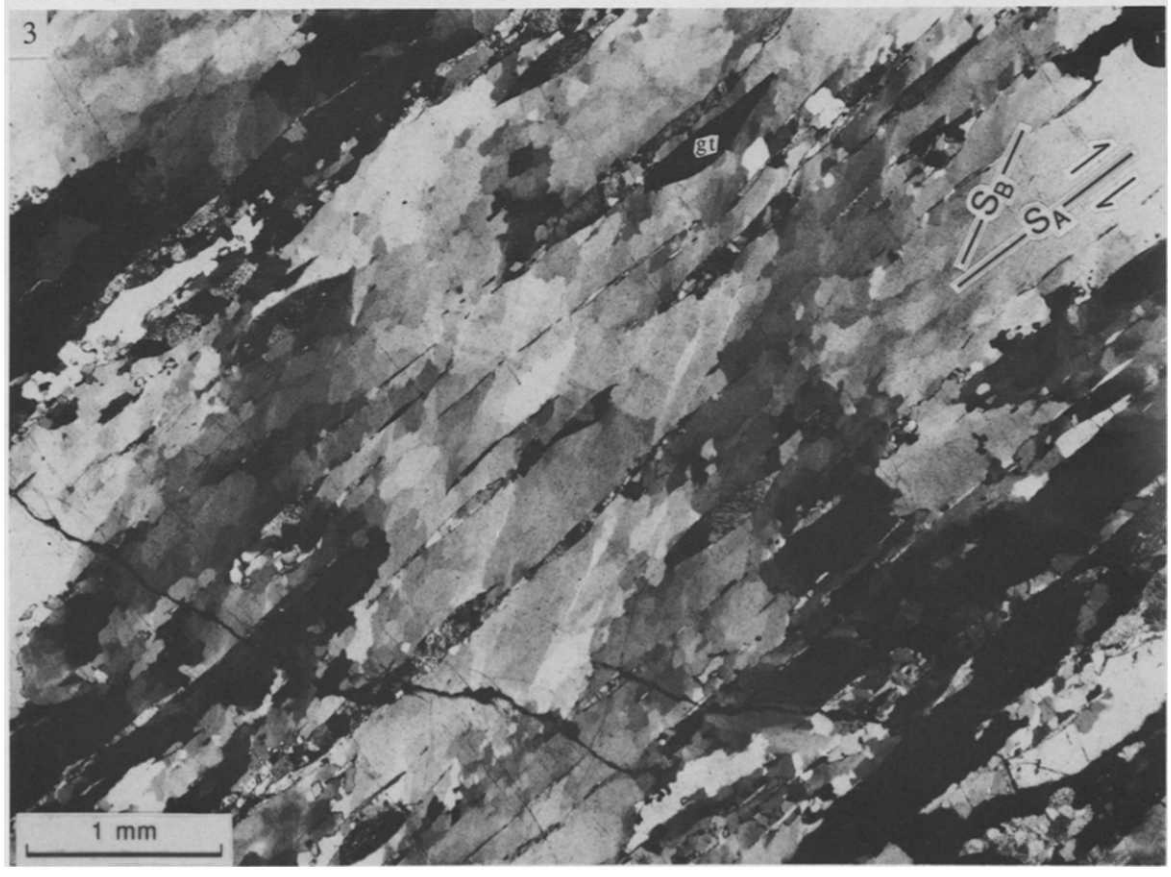

Fig. 2. Typical microstructure of quartz-rich layers in the studied quartzo-feldspathic mylonite (X–Z section). Note the lens-shaped garnet grains and well-developed shape fabrics of quartz and feldspar. gt, garnet; fd, feldspar; qtz, quartz.

Fig. 3. Two types of shape fabrics in the quartz: S_A and S_B. S_A is defined by the bulk orientation of quartz and feldspar ribbons and elongate garnet single crystals while S_B is defined by elongate subgrains and recrystallized new grains of quartz. The angular relationship between S_A and S_B indicates a dextral shear sense. X–Z section.

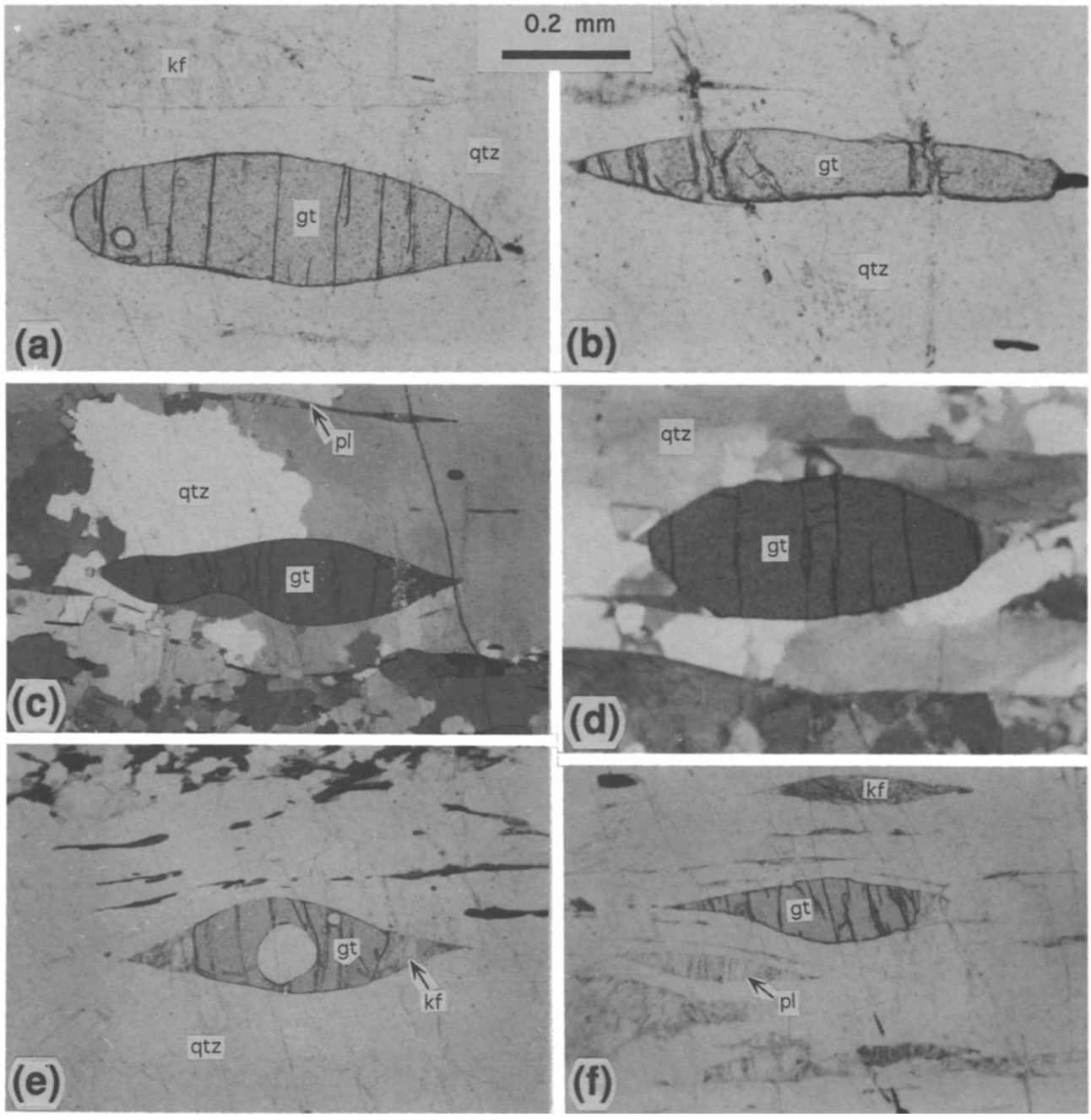

Fig. 4. Photomicrographs of ductilely deformed garnet single crystals in the quartzo-feldspathic mylonite. *X–Z* sections. gt, garnet; kf, K-feldspar; pl, plagioclase; qtz, quartz.

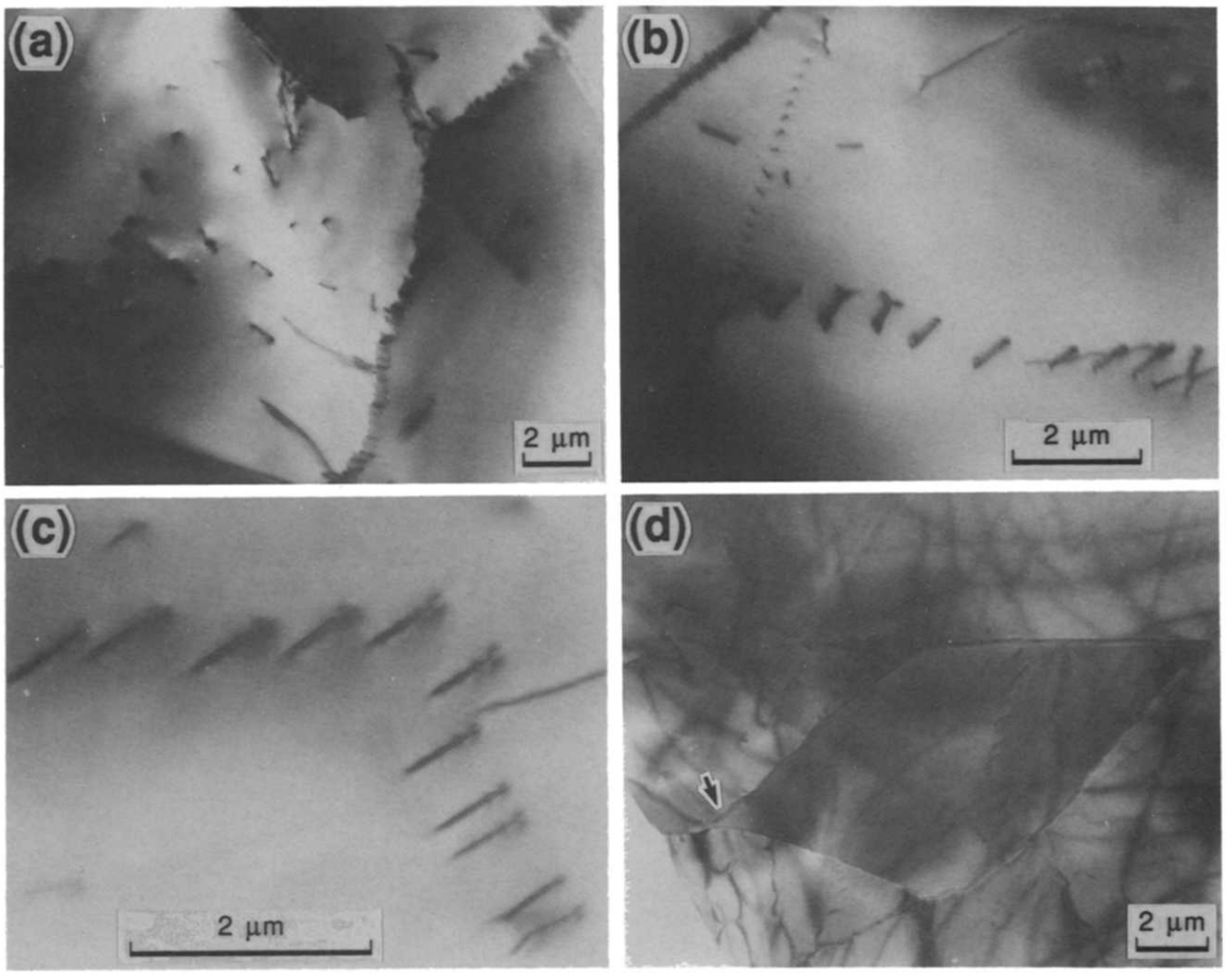

Fig. 5. Bright-field electron micrographs of dislocations in the naturally deformed garnet. (a) Free dislocations. (b)–(d) Subgrain boundaries.

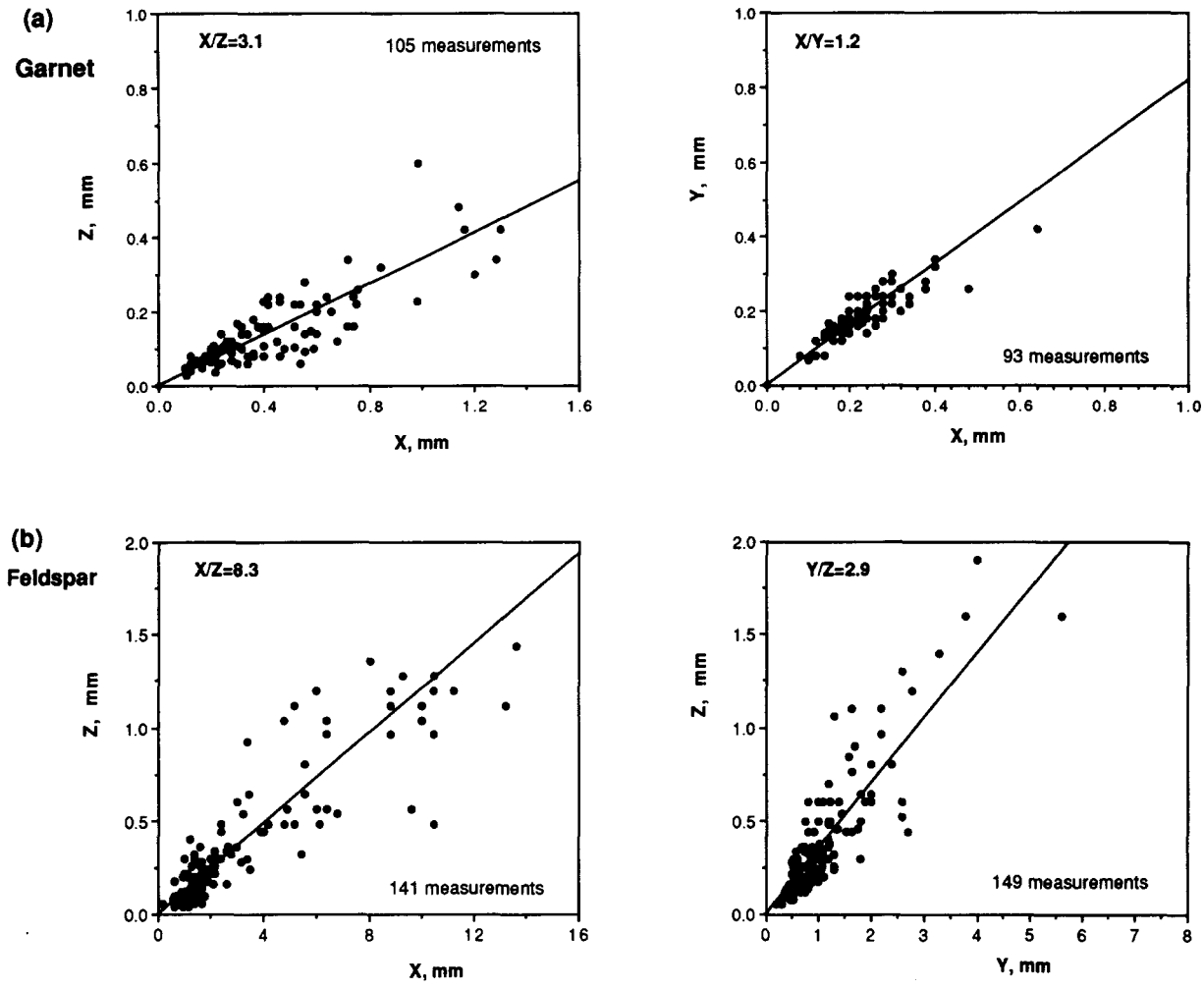

Fig. 6. Dimensions of garnet (a) and feldspar (b) measured in the X–Z and X–Y or Y–Z sections. X is the direction parallel to the stretching lineation; Y parallel to the foliation and perpendicular to the lineation; and Z normal to the foliation. The line on each graph represents an average ratio.

areas indicate free dislocation densities on the order of 5 × 107 cm−2. Subgrain boundaries composed of dislocation arrays (simple tilt walls) (Figs. 6b & c) and, locally, dislocation networks (complex twist boundaries) (Fig. 6d) are extensively developed. These observations indicate a steady-state creep behavior of garnet due to effective dynamic recovery (dislocation climb and cross-slip). Therefore, we consider that the predominant deformation mechanism is recovery-accommodated dislocation creep. On-going work will characterize in detail the dislocation sub-structures.

Feldspar

Both K-feldspar and plagioclase are present as lenticular and/or pinch-and-swell-shaped, mono- and polycrystalline ribbons isolated in the matrix of quartz (Figs 2, 3 and 4a & f). They are elongate in the plane of the foliation and parallel to the extension lineation. The aspect ratio of feldspar lenticular ribbons in the X–Z section ranges from 1 to 14, with an average value of 8.3 while in the Y–Z section it ranges from 1 to 6, with an average value of 2.9 (Fig. 6b). The corresponding Flinn coefficient (k) is equal to 1.02, indicating a non-coaxial plane strain. Cuspate terminations of feldspar (Gower & Simpson 1992) are commonly observed at the sites of quartz–feldspar–quartz three-grain contact. Evidence of intracrystalline deformation, such as large lattice bending, deformation bands, mechanical twins, subgrains and recrystallized new grains (e.g. White & Mawer 1986, 1988, Ji & Mainprice 1988, 1990), are abundant in the feldspars. Exsolutions are common in perthite porphyroclasts with thicker lenticular exsolution lamellae observed near the boundary and with thinner lamellae in the center. These suggests that the feldspar grains were deformed by diffusion-assisted dislocation creep (White & Mawer 1986, 1988). Some relatively short lenses of feldspar (less deformed) have a clear asymmetry with respect to the foliation and lineation, indicating a dextral rotational deformation during ductile deformation of the feldspar.

Quartz

Quartz occurs as ribbon-shaped grains with optical evidence for intracrystalline plastic strain, such as undulate extinction, subgrains and dynamic recrystallization (Figs. 2 and 3). On hand specimen and at outcrop scale, the shape fabric of quartz ribbons is characterized by $X > Y > Z$. In thin sections parallel to the X–Z-plane, two

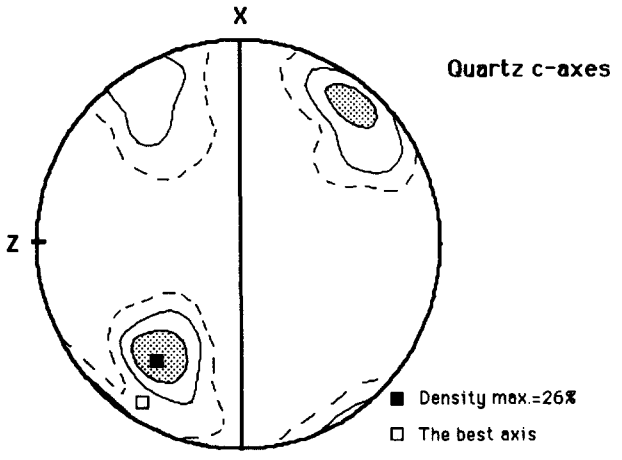

Fig. 7. Quartz *c*-axis preferred orientation in the quartz ribbons. The *X*–*Y* plane (foliation) is the N–S solid line and is perpendicular to the page; the *X*-direction (lineation) is N–S. Contours: 1, 4 and 8%. Highest contour interval shaded. Equal-area projection, lower-hemisphere. 150 measurements.

shape fabrics are visible: S_A and S_B (Law *et al.* 1990) (Fig. 3). S_A is defined by the bulk orientation of quartz grains and is parallel to that defined by elongate garnet and ribbon feldspar and also parallel to the regional foliation in the field. S_B is defined by elongated subgrains and recrystallized new grains in the ribbons. S_B is much less pronounced than S_A and oblique to S_A at an average angle of 25° (Fig. 3). The angular relationship between S_A and S_B (Law *et al.* 1990) indicates dextral non-coaxial shearing.

Quartz *c*-axis orientations measured in the ribbons are clustered around the mineral lineation (Fig. 7). This fabric pattern is consistent with those reported by Lister & Dornsiepen (1982) and Gower & Simpson (1992) and is interpreted as the product of dislocation glide along ⟨*c*⟩ on the prism slip system in quartz at temperatures above 600°C (Blumenfeld *et al.* 1986, Mainprice *et al.* 1986).

Two-dimensional neograin-size (D) is calculated as the diameter of a circle of equivalent area to the measured grain which is often of an elongated shape. Measurements show a mean two-dimensional dynamically recrystallized quartz grain-size of 152 ± 62 μm, suggesting a differential stress during the last deformation of 10 MPa (using the recrystallized grain-size paleopiezometer of Mercier *et al.* 1977). At a supposed strain-rate of 10^{-14} s^{-1}, an average strain rate for shear zones in orogenic regions (Carter & Tsenn 1987), this value of the flow stress suggests a deformation temperature of about 550°C using the flow law of Koch *et al.* (1980) for dry quartz. This implies that the studied neograins and *c*-axis fabric of quartz were formed at upper amphibolite facies conditions at geologically realistic strain-rates.

DISCUSSION: ORIGIN OF FLATTENED GARNETS

The observations demonstrate that garnets in the mylonite are flattened in the foliation plane whereas feldspar and polycrystalline quartz are elongated parallel to the stretching lineation. The origin of oblate garnet may be complex and the following possibilities are discussed.

Shear sliding

Flattened grains of garnet can be produced by shearing of initially equant grains parallel to the foliation (Gregg 1978). The characteristics of the tabular grains formed by this mechanism are: (1) grains are usually angular; (2) if crystal segments have not been displaced much, they can be restored to their original relative positions; and (3) no subgrain boundaries can be formed in the fragments. This mechanism may prevail in strongly anisotropic, low grade metamorphic rocks such as garnet-rich, chlorite–muscovite schists (Gregg 1978). Strong anisotropy caused by platy minerals aligned in the foliation can favor foliation-parallel shearing, and low temperature can prevent rounding the angular corners of garnet segments. This mechanism is highly unlikely for the flattened garnets studied here since the characteristics of (1)–(3) have not been observed.

Anisotropic growth

Anisotropic growth under differential stress within a pre-existing anisotropic structure such as a well-developed foliation has been cited as a mechanism producing oblate grains (Gresens 1966, Blackbrun & Dennen 1968, Powell & MacQueen 1976, Karato & Masuda 1989). At a specific temperature, the rate of growth of garnet depends on the proximity and abundance of garnet components and the ease of diffusivity of components to and from the sites of growth. Therefore one might expect that garnets would grow more rapidly and to a greater size in the foliation surface because chemical mass transfer by Coble diffusion in such a surface is favored with respect to Nabbarro–Herring diffusion in the direction normal to the foliation. Several conditions may favor this process, including (i) large deviatoric stress and (ii) presence of grain-boundary fluids (Karato & Masuda 1989). Dimensionally flattened garnets produced by the above mechanism have been documented from the Kiawa pegmatite of New Mexico, where Gresens (1966) found that straight dodecahedral faces of flattened spessartine garnets are parallel to the muscovite foliation. Blackbrun & Dennen (1968) noted that, in quartzo-feldspathic gneisses from the Grenville Province of southeast Ontario, almandine garnets located in the biotite foliation planes are almost always oblate, whereas the garnets of adjacent quartzo-feldspathic layers are more equidimensional. They also observed that the chemical composition of oblate garnets is different from that of equidimensional ones, although they are separated by only a few millimeters. This shows that diffusion did not occur across compositional layers.

The anisotropic growth of oblate garnets cannot be applied to the Morin shear zone because: (1) no straight

euhedral faces of garnets have been developed in the flattened garnets (Figs. 2–4); (2) biotite is scarce in both the quartz-rich and feldspar-rich layers (Figs. 2–4); and (3) dislocation-recovery structures such as low-angle walls are observed in the garnet (Fig. 5).

Metamorphic reaction

In high-grade rocks, garnet has been interpreted to have nucleated and grown as pseudomorphs after biotite or sillimanite (Blackbrun & Dennen 1968). We indeed found this kind of elongated garnet in other metamorphic rocks, and original features such as (001) cleavages of biotite or {010} of sillimanite were still retained in the pseudomorph. This feature was not observed in the flattened garnets studied here, and thus metamorphic reaction does not seem to be the proper mechanism for the formation of the flattened garnets from the Morin shear zone.

Plastic deformation

Crystal plasticity by dislocation slip accommodated by diffusion has been cited by Dalziel & Bailey (1968) and Ross (1973) for the formation of dimensionally flattened garnets within mylonites from the Grenville Province near Coniston, Ontario, and from the Oliver area in the southern Okanagan Valley of British Columbia, Canada. Using the transmission Laue X-ray technique described by Bailey *et al.* (1958), they found that the crystal structure of these flattened garnets had undergone considerable distortion, although these garnets are still optically isotropic. However, it should be pointed out here that: (i) our garnets seem to be much more dimensionally flattened than their garnets; and (ii) inclusions of quartz and feldspar (see plate 1 in Dalziel & Bailey 1968, fig. 9a in Ross 1973) are abundant within their garnets while such inclusions are rare in those from the Morin area. As inclusions are abundant in the core and rare near the rim of garnets described by Ross, these garnets seem to be formed by anisotropic overgrowth (i.e. overgrowth was rapid in the direction parallel to the foliation and slow perpendicular to the foliation) of precursory grains rich in quartz inclusions. The garnets of Dalziel & Bailey contain many quartz inclusions aligned parallel to the general foliation in the thin section (plate 1 in Dalziel & Bailey 1968). It therefore seems that these garnets are porphyroblasts rather than porphyroclasts.

From crystal structure and dislocation energy considerations, crystals with large Burger's vectors tend to have high Peierls stress and a large resistance to glide. In garnet, which has a b.c.c. crystal structure and very large unit cell, the Burger's vector is large (the shortest Burger's vectors are $a/2\langle 111\rangle$ and $a\langle 100\rangle$, with lengths of about 0.7 and 1.2 nm). In garnet, the 4 co-ordinated cation has approximated 50% covalent character and the common 6- and 8-co-ordinated cations form predominantly ionic bonds (Smith 1982, Allen *et al.* 1987). The ionocovalent bonding also favors a higher lattice resistance to glide, so that the Peierls stress of garnet is particularly high and consequently, the creep strength of garnets is significantly higher than that of other silicates or oxides (Karato 1989).

Most previous deformation experiments on garnet were carried out on synthetic single crystal oxide garnets such as $Gd_3Ga_5O_{12}$ (GGG), $Y_3Al_5O_{12}$ (YAG) and $Y_3Fe_5O_{12}$ (YIG) because of their industrial applications (Rabier *et al.* 1976, Garem *et al.* 1982, Rabier & Garem 1984, Wang & Karato 1991, Wang *et al.* 1991). So far as we are aware, recent creep experiments in Karato's laboratory, University of Minnesota (Wang & Karato personal communication, Liu *et al.* 1992) are the only plastic deformation experiments performed on natural silicate garnets: grossularite, grossularite–almandine, almandine-pyrope and spessartine. The previous results on plastic deformation of garnet can be briefly summarized as follows: (i) flow strength of garnet varies with its chemical composition. At a given temperature and strain-rate, garnets can be arranged in the following order: YAG > GGG > YIG > almandine-pyrope > grossularite > spessartine in terms of flow strength (Wang *et al.* 1991, Liu *et al.* 1992); (ii) in order to generate plastic deformation of garnet by creep at convenient laboratory strain rates ($\dot{\varepsilon} = 10^{-5}$–$10^{-6}$ s^{-1}), a very high temperature is required for silicate (>1050°C) and oxide (>1200°C) garnets. The flow stress is still very high (>300 MPa), even at a temperature close to the melting temperature (T_m) ($T/T_m > 0.9$); and (iii) TEM studies by these authors show that dislocation glide is the main mechanism in garnet single crystals, with $\{110\}\ a/2\ \langle 111\rangle$ as a dominant slip system and $\{110\}\ \langle 100\rangle$ as a secondary slip system (Rabier *et al.* 1979, Garem *et al.* 1982, Smith 1982, Rabier & Garem 1984, Wang *et al.* 1991). An $a/2\langle 111\rangle$ perfect dislocation can be dissociated into two $a/4\ \langle 111\rangle$ partial dislocations that are separated by a stacking fault (Rabier *et al.* 1976, Allen *et al.* 1987). Subgrain boundaries due to diffusion-controlled dislocation climb (dynamic recovery) occurs in high temperature strained garnets (Rabier *et al.* 1979, Garem *et al.* 1982, Rabier & Garem 1984).

A comparison of our optical and TEM observations with available experimental data and theoretical predictions based on crystal structure and dislocation energy considerations suggest that the garnets from the Morin shear zone were deformed at such a high temperature that recovery-accommodated dislocation slip became the main mechanism of deformation. This is why ductilely deformed garnets are rarely described from crustal mylonites.

How could (strong) garnet single crystals be deformed in an interconnected, stress-supporting matrix of (soft) quartz? Theoretical analysis by Freeman & Lisle (1987) shows that during a single deformation event, inclusions stiffer than their matrix will deform into a less oblate shape (higher Flinn coefficient k) than the bulk strain and vice versa. As in the mylonite studied garnet has a more oblate shape than associated feldspar and quartz

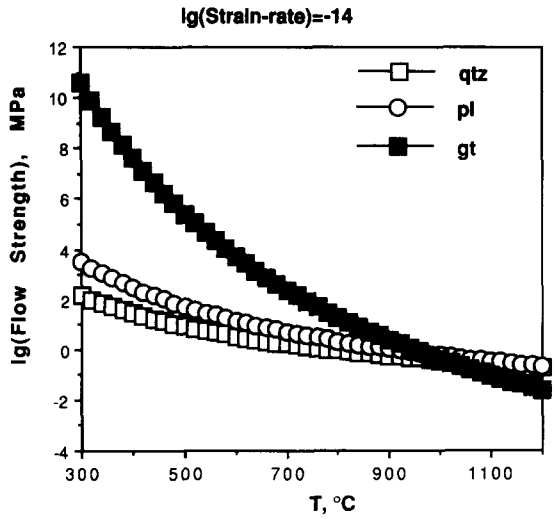

Fig. 8. Flow strength–temperature profiles in the dislocation creep regime for single crystal garnet (almandine–pyrope) (gt), monomineralic aggregates of quartz (qtz) and plagioclase (pl) at a strain-rate of 10^{-14} s^{-1}. For garnet (Alm 68 Prp 20 Grs 12), the flow law parameters $A = 5.84 \times 10^6$ MPa^{-n} s^{-1}, $n = 2.22 \pm 0.10$ and $Q = 485 \pm 30$ kJ mol^{-1} (Wang & Karato personal communication, Liu *et al.* 1992). For quartz, $A = (2.40 + 2.52/-1.24) \times 10^{-7}$ MPa^{-n} s^{-1}, $n = 2.86 \pm 0.18$ and $Q = 149 \pm 29$ kJ mol^{-1} (Koch *et al.* 1980). For plagioclase, $A = (3.27 \pm 1.00) \times 10^{-4}$ MPa^{-n} s^{-1}, $n = 3.2$ and $Q = 238$ kJ mol^{-1} (Shelton & Tullis 1981). Thickness of the curves stands for the maximum error range.

(Fig. 6), it had to be softer than these minerals. On the other hand, the temperatures from 750 to 550°C, under which Morin dextral strike-slip shearing took place (Martignole & Schrijver 1970, Martignole 1992), is too low to cause garnet to be softer than feldspar and quartz. Otherwise, if garnet could be deformed plastically at such a temperature, one would commonly find deformed garnet in garnet-bearing granulite- or upper amphibolite-facies mylonites.

Figure 8 plots the flow strength of quartz, plagioclase and garnet (almandine–pyrope) as a function of temperature at a strain-rate of 10^{-14} s^{-1} when these minerals deform within the dislocation creep regime. It is generally true that dislocation creep prevails in dry and coarse-grained (>50 μm) rocks (e.g. White & Mawer 1986, Tullis & Yund 1991) as indicated by the presence of a lattice preferred orientation, a shape fabric and optical and TEM intracrystalline strain microstructures. The curves shown in Fig. 8 are calculated from the power-flow laws of quartz (Koch *et al.* 1980), plagioclase (Shelton & Tullis 1981) and almandine–pyrope (Alm 68 Prp 20 Grs 12) (Wang & Karato personal communication, Liu *et al.* 1992). Garnet, which is much stronger than quartz and plagioclase at temperatures lower than 700°C, is weaker than plagioclase and quartz above 900°C. It is not surprising that flow strength of solid materials change with temperature. This phenomenon is well known for metal compounds. For example, carbides (TiC) are hard and have a covalent character at low temperature, but become soft and metallic in character at high temperatures (Gilman 1973, Frost & Ashby 1982). At $T/T_m < 0.2$, TiC is several times harder than Si and Ge, and about 50 times harder than Cu, but at $T/T_m = 0.5$, while Si, Ge and Cu retain their strength, the strength of TiC drops to a value similar to that of Cu (Atkins 1973). If the situation shown in Fig. 8 is true, we may postulate a circumstance as follows: at an early stage of tectonic deformation, temperature might have been so high (>900°C) that garnet was softer than its quartz–feldspar matrix. However, the volume fraction of garnet (2–3%) is too low for garnet grains to form an interconnected, stress-supporting network. Therefore, quartz and feldspar would be deformed also ductilely at the same time as garnet but to a lesser extent. On the other hand, stronger quartz and feldspar inclusions within softer garnets remained undeformed. With decreasing temperature, an inversion of flow strength took place and consequently garnet became more rigid with respect to quartz and feldspar. Quartz inclusions thus became protected from further deformation by their garnet armor. This is why the inclusions of quartz and feldspar within the garnet crystals do not show any optical evidence for either intracrystalline strain (e.g. undulatory extinction and lattice bending) or recovery (subgrain boundaries and recrystallization). Ductile deformation of garnet in quartzo-feldspathic mylonites at very high temperatures (≥900°C) also implies that water activity must have been low. If water activity had been high enough to cause partial melting, the differential stress would have become too low (Ji & Mainprice 1986, Dell'Angelo & Tullis 1988) to deform garnet single crystals in a partially molten matrix.

The extremely high temperature required for ductile deformation of garnet (≥900°C) is assumed to be attained in the rocks which were located in the immediate vicinity of the Morin Anorthosite Massif during its intrusion (~1155 Ma). As the anorthosite was most likely emplaced as a highly viscous but buoyant crystal mush (T ≥ 1200°C, Bayly 1976) in the lower crust, ascent of such a mushroom-shaped diapir might (possibly coaxially?) deform its overburden rocks (Dixon 1975). It is at that time that the garnets in the quartzo-feldspathic rocks were deformed. More than 100 Ma later, after the anorthosite had cooled down from magmatic to metamorphic temperatures, non-coaxial flow related to dextral strike-slip movement (~1020 Ma) along the Morin shear zone (Martignole 1992) took place. This lower temperature (750–550°C) deformation thus erased all traces of previous strain in the still ductile quartz–feldspar matrix but not in the currently rigid garnet. During this dextral strike-slip (non-coaxial) shearing, the earlier foliation might have been re-used or most possibly transposed, and the elongate garnet grains behaving as rigid inclusions were firstly rotated toward and then tended to stay close to the flow plane with increasing finite strain of the matrix (e.g. Fernandez *et al.* 1983, Passchier 1987). After a large rotational strain (e.g. $\gamma = 10$) was achieved, the flow plane became closely parallel to the mylonitic foliation. Finally, in the sample studied, quartz deformed more than feldspar because feldspar is stronger than quartz at lower temperature (<700°C).

CONCLUSIONS

Ductilely flattened garnet and rotationally-sheared quartz and feldspar are found to coexist in mylonites from the Morin shear zone. It is difficult to explain the coexistence of these two types of deformations unless changes in rheological properties of garnet vs quartz and feldspar are advocated. It is considered that garnet is more ductile than both quartz and feldspar above 900°C whereas it becomes much stronger than quartz and feldspar at lower temperature (<700°C). Ductile strain recorded by garnet grains first took place at extremely high temperature and was then preserved from further intracrystalline deformation upon cooling down to metamorphic temperatures. It was followed by a considerably large, rotational strain ($\gamma \approx 10$, Martignole 1992) which took place at temperatures straddling the granulite–amphibolite facies conditions.

Feldspar and particularly quartz, which are easily deformed under middle and low temperature conditions, generally cannot record earlier high temperature deformations. Their microstructures only record the last increments of strain. In contrast, deformed garnets may be among the rare minerals able to preserve information about an early, extremely high temperature deformation because they become rigid and escape further deformation below a temperature where quartz and feldspar continue to deform plastically.

Acknowledgements—This study was supported by grants from the FCAR of Québec, NSERC of Canada and Université de Montréal. We would like to thank Z. Wang and S. I. Karato for using their unpublished rheologic data on garnet. Reviews by Drs C. W. Passchier, D. Mainprice and an anonymous reviewer were most helpful. J. C. White, W. Trzcienski, S. Hanmer, P. Zhao and W. M. Schwerdtner are thanked for discussions, R. Veillette for technical assistance with TEM observations, G. Schonbeck for photography, J. P. Bourque for thin sections and M. Demidoff for drawing Fig. 1. This is LITHOPROBE contribution No. 527.

REFERENCES

Allen, F. M., Smith, B. K. & Buseck, P. R. 1987. Direct observation of dissociated dislocations in garnet. *Science* **238**, 1695–1697.

Anderson, D. L. 1989. *Theory of the Earth*. Blackwell, Boston.

Atkins, A. G. 1973. High-temperature hardness and creep. In: *The Science of Hardness Testing and its Research Application* (edited by Westbrook, J. H. & Conrad, H.). American Society for Metals, Metals Park, Ohio, 223–240.

Bailey, S. W., Bell, R. A. & Peng, C. J. 1958. Plastic deformation of quartz in nature. *Bull. geol. Soc. Am.* **69**, 1443–1466.

Bayly, B. 1976. *Introduction à la Pétrologie*. Masson, Paris,

Bell, T. H., Forde, A. & Hayward, N. 1992. Do smoothly curving, spiral-shaped inclusion trails signify porphyroblast rotation? *Geology* **20**, 59–62.

Bell, T. H. & Johnson, S. E. 1989. Porphyroclast inclusion trails: The key to orogenesis. *J. metamorph. Geol.* **7**, 279–310.

Blackbrun, W. H. & Dennen, W. H. 1968. Flattened garnets in strongly foliated gneisses from the Grenville series of the Ganonoque area, Ontario. *Am. Mineral.* **53**, 1386–1393.

Blumenfeld, P., Mainprice, D. & Bouchez, J.-L. 1986. C-slip in quartz from subsolidus deformed granite. *Tectonophysics* **127**, 97–115.

Burton, K. W. & O'Nions, R. K. 1991. High-resolution garnet chronometer and the rates of metamorphic processes. *Earth Planet. Sci. Lett.* **107**, 649–671.

Carstens, H. 1969. Dislocation structures in pyropes from Norwegian and Czech garnet peridotites. *Contr. Miner. Petrol.* **24**, 348–353.

Carstens, H. 1971. Plastic stress relaxation around solid inclusions in pyrope. *Contr. Miner. Petrol.* **32**, 289–294.

Carter, N. L. & Tsenn, M. C. 1987. Flow properties of continental lithosphere. *Tectonophysics* **136**, 27–63.

Christensen, J. N., Rosenfeld, J. L. & De Paolo D. J. 1989. Rates of tectonomorphic processes from rubidium and strontium isotopes in garnet. *Science* **240**, 1465–1469.

Dalziel, I. W. D. & Bailey, S. W. 1968. Deformed garnets in a mylonitic rock from the Grenville Front and their tectonic significance. *Am. J. Sci.* **266**, 542–562.

Dell'Angelo, L. N. & Tullis, J. A. 1988. Experimental deformation of partially melted granitic aggregates. *J. metamorph. Geol.* **6**, 495–515.

Dixon, J. 1975. Finite strain and progressive deformation in models of diapiric structures. *Tectonophysics* **28**, 89–124.

Doig, R. 1991. U–Pb zircon dates of Morin anorthosite suite rocks, Grenville Province, Quebec. *J. Geol.* **99**, 729–738.

Fernandez, A., Feybesse, J. L. & Mezure, J. F. 1983. Theoretical and experimental study of fabrics developed by different shaped markers in two-dimensional simple shear. *Bull. Soc. géol. Fr.* **25**, 319–326.

Freeman, B. & Lisle, R. J. 1987. The relationship between tectonic strain and the three-dimensional shape fabrics of pebbles in deformed conglomerates. *J. geol. Soc. Lond.* **144**, 635–639.

Frost, H. J. & Ashby, M. F. 1982. *Deformation-mechanism Maps: The Plasticity and Creep of Metals and Ceramics*. Pergamon Press, Oxford.

Garem, H., Rabier, J. & Veyssiere, P. 1982. Slip systems in gadolinium gallium garnet single crystals. *J. Mater. Sci.* **17**, 878–884.

Gilman, J. J. 1973. Hardness: A strength microprobe. In: *The Science of Hardness testing and its Research Application* (edited by Westbrook, J. H. & Conrad, H.). American Society for Metals, Metals Park, Ohio, 51–74.

Gower, R. J. W. & Simpson, C. 1992. Phase boundary mobility in naturally deformed, high-grade quartzo-feldspathic rocks: evidence for diffusional creep. *J. Struct. Geol.* **14**, 301–313.

Gregg, W. 1978. The production of tabular grain shapes in metamorphic rocks. *Tectonophysics* **49**, T19–T24.

Gresens, R. L. 1966. Dimensional and compositional control of garnet growth by mineralogical environment. *Am. Mineral.* **51**, 524–528.

Ji, S. & Mainprice, D. 1986. Transition from power law to Newtonian creep in experimentally deformed dry albite. *Eos* **67**, 1235.

Ji, S. & Mainprice, D. 1988. Natural deformation fabrics of plagioclase: Implications for slip systems and seismic anisotropy. *Tectonophysics* **147**, 145–163.

Ji, S. & Mainprice, D. 1990. Recrystallization and fabric development in plagioclase. *J. Geol.* **98**, 65–79.

Ji, S. & Zhao, P. 1993. Location of tensile fracture within rigid–brittle inclusions in ductilely flowing matrix. *Tectonophysics* **220**, 23–31.

Karato, S. 1989. Plasticity-crystal structure systematics in dense oxides and its implications for the creep strength of the earth's deep interior: a preliminary result. *Phys. Earth & Planet. Interiors* **55**, 234–240.

Karato, S. & Masuda, T. 1989. Anisotropic grain growth in quartz aggregates under stress and its implication for foliation development. *Geology* **17**, 695–698.

Koch, P. S., Christie, J. M. & George, R. P. Jr. 1980. Flow law of wet quartzite in the alpha quartz field. *Eos* **61**, 376.

Law, R. D., Schmid, S. M. & Wheeler, J. 1990. Simple shear deformation and quartz crystallographic fabrics: a possible natural example from the Torridon area of NW Scotland. *J. Struct. Geol.* **12**, 29–45.

Lister, G. S. & Dornsiepen, U. F. 1982. Fabric transitions in the Saxony granulite terrain. *J. Struct. Geol.* **4**, 81–92.

Lister, G. S. & Williams, P. F. 1983. The partitioning of deformation in flowing rocks masses. *Tectonophysics* **92**, 1–33.

Liu, B., Wang, Z., Fujino, K. & Karato, S. 1992. High-temperature creep of garnets, III: Alumino-silicate garnets and the rheology of the transition zone. *Eos* **73**, 378.

Mainprice, D., Bouchez, J. -L., Blumenfeld, P. & Tubia, J. M. 1986. Dominant *c*-slip in naturally deformed quartz: implications for dramatic plastic softening at high temperature. *Geology* **14**, 812–822.

Martignole, J. 1992. The Morin terrane revised. In: *Abstract For Abitibi-Grenville LITHOPROBE Workshop* (Montréal, Canada), 15.

Martignole, J. & Friedman, R. M. 1993. Age constraints on terrane assembly along the Montréal-Val-d'Or transect, Grenville Province (Québec), LITHOPROBE Workshop (extended abstract).

Martignole, J. & Schrijver, K. 1970. Tectonic setting and evolution of the Morin Anorthosite, Grenville Province, Quebec. *Bull. geol. Soc. Finland* **42**, 165–209.

Mercier, J.-C., Anderson, D. A. & Carter, N. L. 1977. Strain in the lithosphere: inferences from steady-state flow of rocks. *Pure & Appl. Geophys.* **115**, 199–226.

Passchier, C. W. 1987. Stable positions of rigid objects in non-coaxial flow-a study in vorticity analysis. *J. Struct. Geol.* **9**, 679–690.

Passchier, C. W., Trouw, R. A. J., Zwart, H. J. & Vissers, R. L. M. 1992. Porphyroblast rotation: eppur si muove? *J. metamorph. Geol.* **10**, 283–294.

Parthasarathy, T. A., Mah, T. I. & Keller, K. 1992. Creep mechanism of polycrystalline yttrium-aluminium garnet. *J. Am. Ceram. Soc.* **75**, 1756–1759.

Powell, D. & MacQueen, J. A. 1976. Relationships between garnet shape, rotational inclusion fabrics and strain in some Moine metamorphic rocks of Skye, Scotland. *Tectonophysics* **35**, 391–402.

Rabier, J. & Garem, H. 1984. Plastic deformation of oxides with garnet structure. In: *Materials Science Research, Vol.* 18 (edited by Tressler, R. E. & Bradt, R. C.). Plenum Press, New York, 187–198.

Rabier, J., Veyssière, P., Garem, H. & Grilhé, J. 1979. Sub-grain boundaries and dissociation of dislocations in yttrium iron garnet deformed at high temperatures. *Phil. Mag.* **A39**, 693–708.

Rabier, J., Veyssière, P. & Grilhé, J. 1976. Possibility of stacking faults and dissociation of dislocations in the garnet structure. *Phys. Stat. Sol.* **A35**, 259–268.

Ringwood, A. E. 1975. *Composition and Petrology of the Earth's Mantle*. McGraw-Hill, New York.

Rivers, T., Martignole, J., Gower, C. F. & Davidson, A. 1989. New tectonic divisions of the Grenville Province. *Tectonics* **8**, 63–84.

Ross, J. V. 1973. Mylonitic rocks and flattened garnets in the Southern Okanagan of British Columbia. *Can. J. Earth Sci.* **10**, 1–17.

Shelton, G. L. & Tullis, J. 1981. Experimental flow laws of crustal rocks. *Eos* **62**, 396.

Smith, B. K. 1982. Plastic deformation of garnets: mechanical behavior and associated microstructure. Unpublished Ph.D thesis, University of California, Berkeley.

Spear, F. S. & Selverstone, J. 1983. Quantitative *P–T* paths from minerals: Theory and tectonic applications. *Contr. Miner. Petrol.* **83**, 348–357.

Spry, A. 1983. *Metamorphic Textures*. Pergamon Press, New York.

Tullis, J. & Yund, R. A. 1991. Diffusion creep in feldspar aggregates: experimental evidence. *J. Struct. Geol.* **13**, 987–1000.

van Roermund, H. L. M. 1989. High-pressure ultramafic rocks from the Allochthonous Nappes of the Swedish Caledonides. In: *The Caledonide Geology of Scandinavia* (edited by Gayer, R. A.). Graham & Trotman, London, 205–219.

Wang, Z. & Karato, S. 1991. High temperature plasticity of garnet. *Eos* **72**, 287.

Wang, Z., Karato, S. & Fujino, K. 1991. High temperature plasticity of garnets: II. *Eos* **72**, 452.

White, J. C. & Mawer, C. K. 1986. Extreme ductility of feldspars from a mylonite, Parry Sound, Canada. *J. Struct. Geol.* **8**, 133–143.

White, J. C. & Mawer, C. K. 1988. Dynamic recrystallization and associated exsolution in perthites: evidence of deep crustal thrusting. *J. geophys. Res.* **93**, 325–337.

Yardley, B. W. D. 1977. An empirical study of diffusion in garnet. *Am. Mineral.* **62**, 793–800.